

Computational Solution to the Problems of Projectile Motion under Significant Linear Drag Effect

Annasi Ayubu Said^{1*}, Msafiri Mmasa Mshewa², Grant Charles Mwakipunda³, Mbega Ramadhani Ngata³, Elfakiri Ali Mohamed⁴

¹Department of Physics, School of Mathematics and Physics, China University of Geosciences, Wuhan, China

²Department of Physics, Faculty of Natural Science, Abdulrahman Al-Sumait University (Sumait-University), Zanzibar, Tanzania

³Key Laboratory of Tectonics and Petroleum Resources Ministry of Education, China University of Geosciences, Wuhan, China

⁴Department of Economic, Zanzibar University, Zanzibar, Tanzania

Email: *annasiayubu@gmail.com

How to cite this paper: Said, A.A., Mshewa, M.M., Mwakipunda, G.C., Ngata, M.R. and Mohamed, E.A. (2023) Computational Solution to the Problems of Projectile Motion under Significant Linear Drag Effect. *Open Journal of Applied Sciences*, 13, 508-528. <https://doi.org/10.4236/ojapps.2023.134041>

Received: March 3, 2023

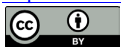
Accepted: April 18, 2023

Published: April 21, 2023

Copyright © 2023 by author(s) and Scientific Research Publishing Inc.

This work is licensed under the Creative Commons Attribution International License (CC BY 4.0).

<http://creativecommons.org/licenses/by/4.0/>



Open Access

Abstract

This paper investigates the computational solution to the problem of projectile motion under a significant linear drag effect. The drag force acting on the particle within the medium of propagation is proportional to the cross-section area of the projectile, the velocity of the particle, and the medium's density. From zero air resistance force (vacuum) the problems are well known with solutions, but with air resistance (drag force) the problems have no exact analytical solutions which lead to most of the significant scientific research works using numerical methods. Therefore, this study aims to present the analysis of the computational modelling of drag force exerted by the surrounding medium on the linear motion. However, the horizontal and vertical components of differential equations of motion were derived and characterized from the solutions governed by Newton's 2nd law of motion. The baseball features were presented as the projectile (object) in this work. In addition, the numerical computational results were received from FreeMat. The results were discussed and compared with those from the vacuum. Moreover, the displacements, velocities, range, and trajectories of the projectile were all discussed and a conclusion was made.

Keywords

Drag Force, Air Resistance, Projectile, Newton's Law

1. Introduction

Projectile motion involves the projectile (object) that is thrown into space. It

firstly experiences gravitational force along its path called a trajectory. However, Galileo was the first person to properly describe projectile motion theory which consists of horizontal and vertical components [1]. After adjacent observation, Galileo resolved that the first vertical force acting on a projectile was gravity (9.8 m/s^2). He also pragmatic that the horizontal motion of the projectile was constant and followed the law of inertia which state that “an object will maintain its state of rest or uniform motion providing no outward force acts upon the object”. Galileo also explained that when combining the horizontal and vertical motion of an object, they form the mathematical curve known as the parabola [1] [2] [3], as the results of supplementary considerable effort came to spot the great significance of his discovery. He believed that the percussive effect of falling objects shows the instantaneous velocity increase with the increase of distance from free fall. Also, in his manuscript notes (fol. 128) as explained in [4] [5] he claimed that mean velocity increases with the square of the distance fallen. This meant that the mean velocity seems to be proportional to the square of the final instant velocity of an object. In this work, the computational solution for the projectile motion problems by taking into account linear drag effects was analysed by FreeMat software.

Previous researchers have investigated projectile motion by considering numerous factors with various methodologies. The study conducted by Ebaid [6] provided a fractional calculus explanation of projectile motion before comparing it with experimental results from Charles [7]. Similarly, he derived various formulas for analytical solutions. In [8], an analytical solution for the speed of a projectile as a function of time has been found in the form of a ratio of two series expansions. In [9], an approximation of a solution has been found for the equations of how a projectile moves in air resistance over short and long periods of time. In [10], the same thing has been done for low-angle ballistics. More analytical estimates have also been thought about [11] [12] [13]. [13] [14] [15] [16] have looked at how the initial spin of a ball and the resulting lift force change the way the ball moves when it is thrown. [17] [18] looked about the bio-ballistics of small projectiles, which is used to explain how insects jump and how plants shoot their seeds. Also, Zhao [19] used the same Lambert W function and concluded that the higher the projection point, the wider the range and slighter optimal angle it become. Moreover, [10] [19] [20] have looked into how the Lambert W function used to figure out how a projectile moves when it has linear drag, while in [21] [22] examine the Excel spreadsheets that castoff the simulation of projectile motion with air resistance before [8] [23] [24] [25] [26] talk about the history of projectile motion in the real world. [23] [27] [28] wrote about the results of experiments where sports balls were used as projectiles. Using a nonlinear drag model with a drag coefficient that changes with Mach number. Taylor *et al.* [29] came up with approximate formulas for spherical projectiles fired from shotguns or muzzleloaders.

In some classical textbooks on mechanics and physics also explained about different parts of how projectiles move [30] [31] [32]. Furthermore, the non-elastic

bouncing of a spherical ball in the presence of quadratic drag has been looked at in terms of sports balls [33]. Linear and quadratic damping models have also been used to study pendulums with big swings, as was recently reviewed in [34]. The overview of a point mass with quadratic resistance was discussed analytically and gave the solution to equations of motion [8]. Due to its application in different aspects such as sports, the projectile motion has been used and contributed a lot in sports science like football, netball, basketball, etc., as it was explained in [35] [36] [37] [38]. Furthermore, Lubarda [39] reviewed the influence of wind on projectile motion by considering the spherical projectile in the existence of linear and nonlinear drag force and stated the results can only be obtained numerically because the analytical solution encounter coupled differential equation of motion that cannot be solved, though in the situation of quadratic drag, proper angle parameter and velocity has closed type relationship. Due to this case, this paper will present the desired degree of accuracy that focus on providing mathematical and computational solutions on the model equation on linear projectile motion. Furthermore, the importance of these results will include both research and pedagogical contributions of curiosity for applied physics and engineering education.

The difference between the effects of air resistance on projectile motion can be shown in the **Figure 1**, the trajectory line with air resistance experience opposing force that makes it lose its momentum. Furthermore, the whole process of motion is characterized by the solution which is governed by Newton's 2nd law of motion [40]. From **Figure 1** we can resolve all forces acting on the moving object (projectile) by finding the summation of entire forces acting on the projectile.

Now for the linear drag motion, the projectile encounter gravitation and drag force both at once which act in the opposite direction of motion. On the other hand, the trajectory without air resistance experience only one force (gravity) acting on the projectile pointing toward the ground. To this fact, its maximum height (h), maximum range (R_{vac}), and the total time for the whole motion are

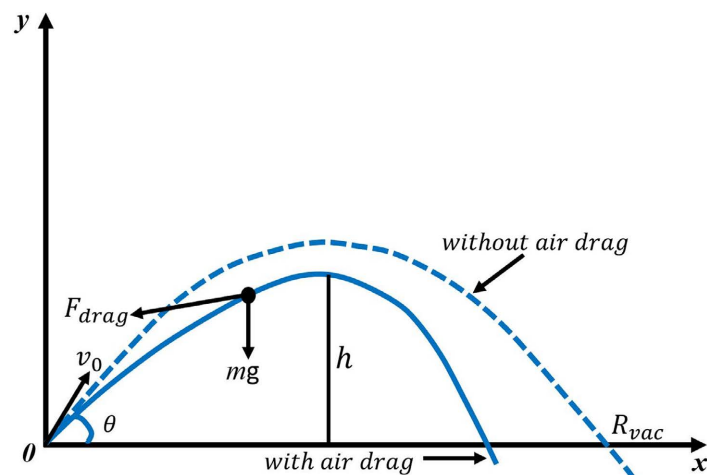


Figure 1. The two trajectories of projectile motion show the effects of air resistance (solid line) and without air resistance (dashed line) during projection [41].

expected to be larger than those with air resistance.

Throughout this study, some initial conditions were set to be constant and were used for each part wherever needed. At STP (Standard Temperature and Pressure), $B = 1.6 \times 10^{-4} \text{ N} \cdot \text{s}/\text{m}^2$ (constant of the linear motion) [42], and since the projectile used was spherical then the linear factor is the diameter (D) and was set to be 7.5 cm, mass of the baseball $m = 145 \text{ g}$ [43] and gravity $g = 9.81 \text{ m}/\text{s}^2$. The FreeMat software [44] used in this study is an open-source alternative to commercial programs like IDL (Interactive Data Language) from Research System, and MATLAB software from MathWorks. It was used to run all simulations for this study, and different analytic properties were gladly discussed. Scripting languages from it tend to be quicker and simpler to program in than more structured and compiled languages like C and C++. However, a script requires more time to execute than a compiled program because each instruction is firstly handled by another program (requiring extra instructions) rather than the basic instruction processor directly [45] [46] [47]. Mathematical expressions were driven, and simple code models were generated which yield the results which certified all conditions as far as linear air resistance is concerned.

The rest part of this work is arranged as follows; by considering the properties of the projectile used, the formulation of equations of projectile motion under linear drag force with horizontal and vertical components governed by Newton's second laws of motion was derived and discussed in section 2. In section 3, computational results of the different functions derived in section 2 were presented. In this section, we also presented, discussed, and compared the results of projectile motion with and without drag force. Also, the proof that the trajectory path of the projectile lies between the exact trajectory was discussed as in Galileo's parabolic trajectory. The conclusion and summary of this work appear in section 4.

2. Methodology

In this section, the formulation of equations of projectile motion under linear drag force is presented. Therefore, In the case of linear drag, air resistance will be added as the factor to the proposed solution. Gravity and air resistance are two forces that the projectile must contend with. When moving at a speed below the sound's speed in the air, the drag may be around;

$$F_{drag} = a + bv + cv^2 + dv^3 + \dots \quad (1)$$

where v is the velocity of the projectile motion. a , b , c and d are the dimensionless constants of the drag coefficient that depends on the shape of the projectile. At low v , the term with cubic and above can be ignored due to a very small number, and $F_{drag} = 0$.

If we let $v = 0$, and $a = 0$ from (1), then take us to get (2)

$$F_{drag} = a + bv + cv^2 \quad (2)$$

Now, from Newton's 2nd Law applied to cartesian coordinate, projectile mo-

tion with linear drag will be given as (3) and after inserting it with (2) yield (4).

$$m\ddot{r} = \sum \text{Force} \quad (3)$$

Since there are two forces, weight (mg) and drag force ($-bv$) which act in opposite directions for the general motion, and $\ddot{r} = \dot{v}$ then (3) can be written as the first-order differential equation for v then turn out to be Equation (4). For horizontal motion there will be no gravity, then Equation (4) take us to Equation (5).

$$m\dot{v} = mg - bv \quad (4)$$

$$m\dot{v} = -bv \quad (5)$$

2.1. Horizontal Motion

For the horizontal motion, the separation of variables allows an easy solution for the differential Equation (5) above.

$$\begin{aligned} m\dot{v} &= -bv \quad \text{since} \quad m\dot{v} = m \frac{dv_x}{dt} \\ m \frac{dv_x}{dt} &= -bv_x \rightarrow \frac{dv_x}{v_x} = \frac{-b}{m} dt \\ \int_{v_0}^{v_x} \frac{1}{v_x} dv_x &= \int_0^t \frac{-b}{m} dt, \\ v_x &= v_0 e^{\left(\frac{-b}{m}\right)t} \end{aligned} \quad (6)$$

For the v_0 of both horizontal and vertical can be obtained when we resolve components in **Figure 1** between v_0 and θ along the x and y direction and become as,

$$v_0(x) = v_0 \cos \theta \quad \text{and} \quad v_0(y) = v_0 \sin \theta \quad (7)$$

Then, Equation (6) becomes (8) after inserting (7),

$$v_x = v_0 \cos \theta e^{\left(\frac{-b}{m}\right)t} \quad (8)$$

Where the coefficient $b = BD$, B constant of the linear motion, and D diameter of the spherical object.

Since $\frac{m}{b} = \tau$ (tau) then,

$$v_x = v_0 \cos \theta e^{\frac{-t}{\tau}} \quad (9)$$

The solution from Equation (9) above can be obtained by separating the variables, then integrating Equation (10) to yield Equation (11)

$$\frac{dx}{dt} = v_0 \cos \theta e^{\frac{-t}{\tau}} \quad (10)$$

$$\int_{x_0}^x dx = \int_0^t v_0 \cos \theta e^{\frac{-t}{\tau}}$$

$$x = x_0 + v_0 \cos \theta \left(-\tau e^{\frac{-t}{\tau}} + \tau \right)$$

$$x(t) = x_0 + v_0 \cos \theta \tau \left(1 - e^{\frac{-t}{\tau}} \right) \quad (11)$$

Where t is the time taken by an object (projectile) to travel from a distance x_0 to x horizontally.

2.2. Vertical Motion

For the vertical motion, the object (projectile) is considered as a free fall, and its acceleration is considered to be constant [48] since the magnitude of the velocity slowly reduced to zero such that $mg > bv_y$ when approach to maximum height before it turn downward.

At that point, the projectile will start to attain velocity while the drag force rises until it becomes similar to gravitational force as shown in **Figure 2**. During this time as we recall Equation (4) in the y -direction, the equation of motion become as;

$$0 = mg - bv_y$$

$$v_{term} = \frac{mg}{b} \quad (12)$$

For vertical motion, $mg = -bv_{term}$ since the motion of the projectile is reversed to $+y$ to be upward [49]. Due to this reason, we insert Equation (12) to (4) which takes as to (13)

$$m\dot{v}_y = bv_{term} - bv_y$$

$$m \frac{dv_y}{dt} = -b(v_y - v_{term}) \quad (13)$$

Then, separate variables and integrate them from Equation (13).

$$\int_{v_{y0}}^{v_y} \frac{dv_y}{v_y - v_{term}} = \int_0^t \frac{-b}{m}$$

$$v_y = v_{term} + (v_{y0} - v_{term}) e^{\frac{-t}{\tau}} \quad (14)$$

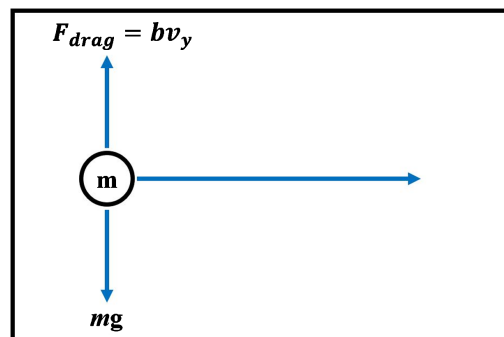


Figure 2. The two forces (gravity and drag force) acting on the projectile.

where $v_{y_0} = v_0 \sin \theta$ for vertical motion and the special case is when $v_{y_0} = 0$ as the projectile is dropping from rest, then Equation (15) is revealed.

$$v_y(t) = v_{term} \left(1 - e^{-\frac{t}{\tau}} \right) \quad (15)$$

where τ (tau) is the characteristic time as defined in [9], while v_{term} as defined in Equation (12). Therefore, we can have the combined relation from the two factors as;

$$v_{term} = g\tau \quad (16)$$

The vertical displacement which is the function of time can be obtained by integrating Equation (14)

$$\int_{y_0}^y dy = \int_0^t \left[v_{term} + (v_{y_0} - v_{term}) e^{-\frac{t}{\tau}} \right] dt$$

$$y = v_{term} t + (v_{y_0} - v_{term}) \tau \left(1 - e^{-\frac{t}{\tau}} \right) \quad (17)$$

Since the vertical motion $v_{y_0} = v_0 \sin \theta$, then Equation (17) become as;

$$y(t) = v_{term} t + (v_0 \sin \theta - v_{term}) \tau \left(1 - e^{-\frac{t}{\tau}} \right) \quad (18)$$

The vertical position in Equation (18) can be modified for the projectile headed upwards rather than downward by replacing v_{term} by $-v_{term}$. The aim is to eliminate t in equations (11) and (18) by transforming the system such that at $t = 0$ and $x_0 = 0$ it becomes as follows;

$$y = v_{term} \tau \ln \left(1 - \frac{x}{v_{x_0} \tau} \right) + (v_0 \sin \theta + v_{term}) \tau \frac{x}{v_{x_0} \tau} \quad (19)$$

where $v_{x_0} = v_0 \cos \theta$ and $\tau \ln \left(1 - \frac{x}{v_{x_0} \tau} \right) = -t$ as it was subjected from Equation (11) and substituted to (18), then upon rearranging this become as follow

$$y = \left(\frac{v_0 \sin \theta + v_{term}}{v_0 \cos \theta} \right) x + v_{term} \tau \ln \left(1 - \frac{x}{v_0 \cos \theta \tau} \right) \quad (20)$$

Here θ , v_0 and x , all are the initial condition to be set for the solution to Equation (20) to meet the trajectory. It can also be called the function for the projectile's path in terms of x .

Refer to Equation (19) as we let R be such value of x and $y = 0$, then the equation will be seen as a non-linear solution that is not possible to solve however, it can be solved numerically or

$$\left(\frac{v_0 \sin \theta + v_{term}}{v_{x_0}} \right) R + v_{term} \tau \ln \left(1 - \frac{R}{v_{x_0} \tau} \right) = 0 \quad (21)$$

with approximation. To guide the scenario in case of no air resistance or vacuum see **Figure 1**.

$$R_{vac} = \frac{2v_{x_0} v_{y_0}}{g} \quad (22)$$

Now the question is, how is the solution in this case of linear drag modified in form of that of the vacuum case? In most cases, if the air resistance is small, make $\frac{R}{v_{x_0} \tau}$ small. Thus, it involves the Taylor series to approximate the logarithmic term to a polynomial, see [50] [51] [52] [53] for more knowledge on Taylor expansion.

$$\ln(1-\varepsilon) \cong -\left(\varepsilon + \frac{1}{2}\varepsilon^2 + \frac{1}{3}\varepsilon^3 + \dots\right) \quad (23)$$

Therefore,

$$\ln\left(1 - \frac{R}{v_{x_0} \tau}\right) = -\left(\frac{R}{v_{x_0} \tau} + \frac{1}{2} \frac{R^2}{v_{x_0}^2 \tau^2} + \frac{1}{3} \frac{R^3}{v_{x_0}^3 \tau^3} + \dots\right) \quad (24)$$

With this approximation, Equation (21) becomes as follows,

$$\frac{v_0 \sin \theta + v_{term}}{v_{x_0}} R - v_{term} \tau \left(\frac{R}{v_{x_0} \tau} + \frac{1}{2} \frac{R^2}{v_{x_0}^2 \tau^2} + \frac{1}{3} \frac{R^3}{v_{x_0}^3 \tau^3} + \dots\right) = 0 \quad (25)$$

Then, $R = 0$ is one of the solutions, the other solution comes from the term in the parenthesis equated to zero.

$$\frac{v_{y_0}}{v_{x_0}} - \frac{1}{2} \frac{R v_{term}}{v_{x_0}^2 \tau} - \frac{1}{3} \frac{R^2 v_{term}}{v_{x_0}^3 \tau^2} = 0 \quad (26)$$

$$\text{Since } \tau = \frac{m}{b}; \text{ then, } v_{term} = \frac{mg}{b} \Rightarrow \frac{v_{term}}{\tau} = g \quad (27)$$

Multiplying Equation (26) by $v_{x_0}^2$ and use the factor in Equation (27), then it yields us to (28) upon rearranging,

$$R = \frac{2v_{x_0} v_{y_0}}{g} - \frac{2}{3v_{x_0} \tau} R^2 \quad (28)$$

From the second term of the above, for low air resistance, τ is very large and to the first approximation $\frac{2v_{x_0} v_{y_0}}{g} = R_{vac}$. Then, for some factors, we consider the trigonometric relation $2v_0 \cos \theta \sin \theta = \sin(2\theta)$, $v_{x_0} = v_0 \cos \theta$ and $v_{y_0} = v_0 \sin \theta$ as expected from introductory Mechanics.

$$R \cong \frac{2v_{x_0} v_{y_0}}{g} = R_{vac}$$

$$R_{vac} = \frac{v_0^2 \sin(2\theta)}{g} \quad (29)$$

From the second term of Equation (28), it is considered to be a correction factor from the vacuum case to improve the approximation.

$$R = R_{vac} - \text{correction}(R_{vac}) \text{ then,}$$

$$R = R_{vac} \left(1 - \frac{4}{3} \frac{v_0 \sin \theta}{v_{term}} \right) \quad (30)$$

This can only be valid when $v_0 \ll v_{term}$, where v_{term} is the terminal velocity, R_{vac} is the range in a vacuum where no air resistance. For the very small air resistance, the range $R \approx R_{vac}$, but due to the correction factor always makes R smaller than R_{vac} and depends on $\frac{v_0 \sin \theta}{v_{term}}$.

3. Results and Discussion

In this study, the linear air resistance models were developed using FreeMat-4.2. We have considered truthful and correct models to model the motion of projectiles like baseballs in both vacuum and air resistance.

3.1. Horizontal Velocity and Displacement

In the horizontal component, the projectile attains its velocity and displacement upon its weight (mg) and is subjected to drag force ($-bv$) which is proportional to its velocity [54]. From Equation (9), one can find the horizontal velocity of the projectile at any given time (t) with any projection angle respectively. Its solution is presented in **Figures 3(a)-(c)**. Since the horizontal velocity (v_x) in linear drag depends on the speed of projection (v_0) which is also known as initial velocity and it tends to slow down depending on time [55] [56] but as $t \approx \infty$, the velocity tends to be zero. The effect of the initial velocity fades with time with a decay rate determined by the characteristic time. The more drag, the faster the initial velocity becomes insignificant in determining the motion.

Since the horizontal displacement has to be in function of time obtained by integration of the velocity, we were required to start with an equation of the linear velocity. That's to say, from the equation of horizontal velocity (9) we can find the horizontal displacement. As in Equation (11) after the separation of variables and integration, its solution was presented in **Figure 4** and compared with the solution from Equation (31) without drag force.

$$x(t) = v_0 \cos \theta t \quad (31)$$

Since its horizontal displacement, in some cases angle theta (θ) = 0 and $x_0 \geq 0$. This means that the projectile did not travel to any vertical component, thus making the gravity have no effects during horizontal motion as discussed in [55]. From **Figure 4**, the red line experiences the drag force as compared with the black line (without drag force) which depends only on the horizontal component of initial velocity and flight time.

3.2. Vertical Velocity and Displacement

The terminal velocity (v_{term}) of the projectile will be attained if it accelerates for the time τ , [57] at constant acceleration g . Since the acceleration is less than g , due to the drag force opposing the direction, then the dropping does not relatively

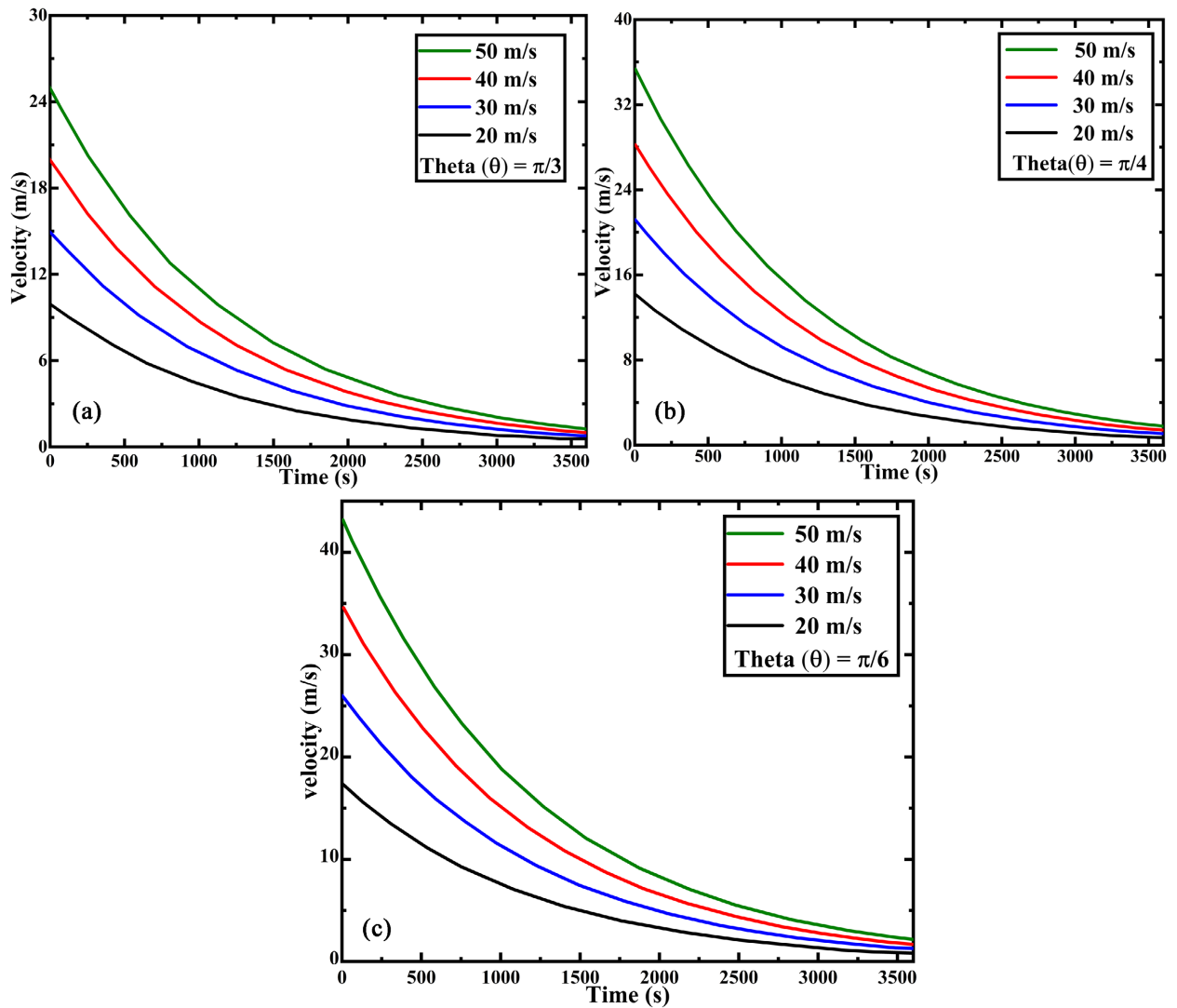


Figure 3. The horizontal velocity of different projection angle (θ) in a ($\pi/3$), b($\pi/4$) and c($\pi/6$).

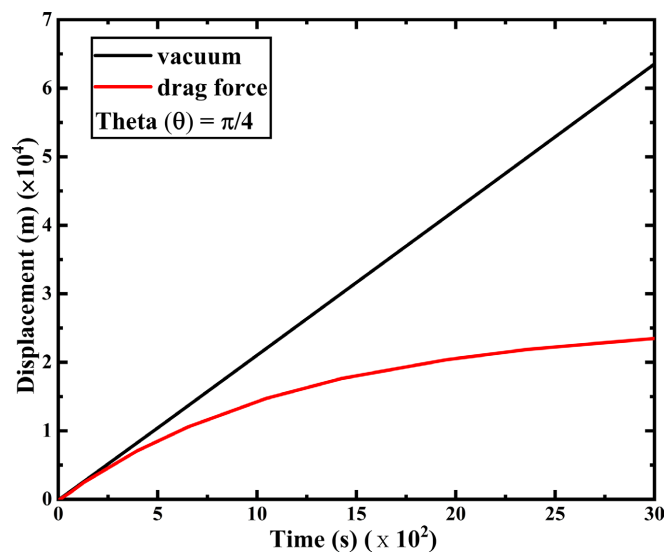


Figure 4. Horizontal displacement (at any given time) with drag force (air resistance) and vacuum.

attain v_{term} after time τ as explained in [58].

From Equation (18), the results in **Figure 5** and **Figure 6** show that, as $t \rightarrow \infty$, $v_y(t) = v_{term}$. And as $t = \tau$, the projectile motion has reached

$$v_y = v_{term} \left(1 - e^{-\frac{t}{\tau}} \right) = 0.63v_{term}, \text{ while at } t = 3\tau, \text{ the velocity of the projectile motion}$$

has reached 95% of v_{term} . It was explained [39] that, this tendency of velocity as a function of characteristic time [9], would be predictable for an object released from rest in a viscid medium wherever the resistance remained proportional to velocity.

The variation of angle theta (θ) and initial velocity (v_0) as in **Figure 6** with terminal velocity (v_{term}) = 1.854×10^4 m/s show that at (b) the displacement is

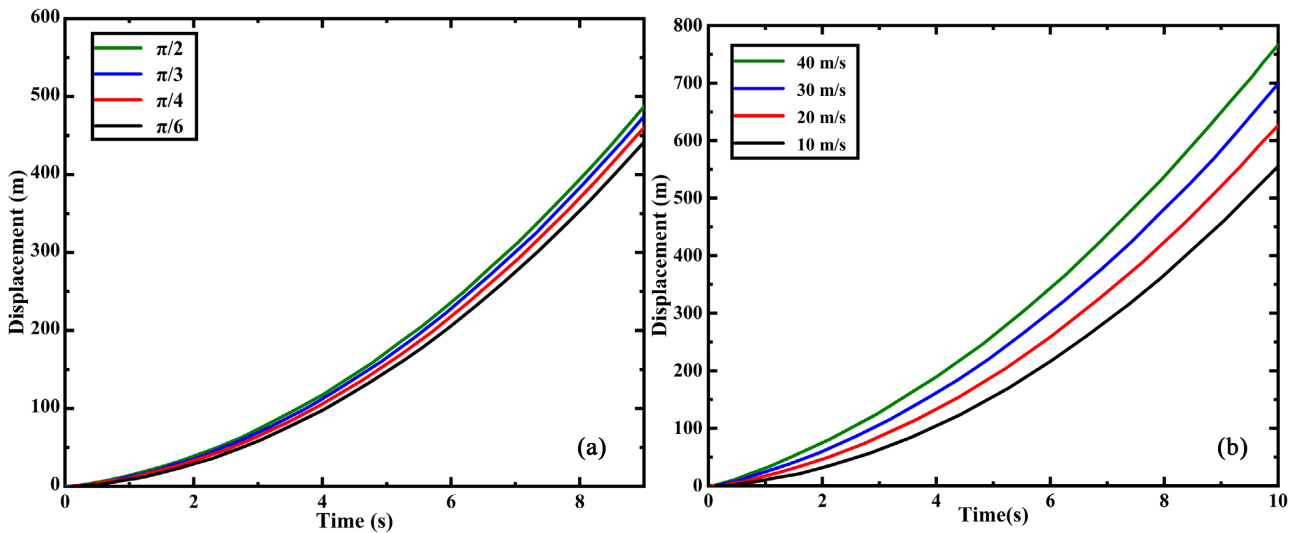


Figure 5. The vertical displacement with (a) variation of theta (θ) at initial velocity (V) = 10 m/s, (b) variation of the initial velocity at theta (θ) = $\pi/2$.

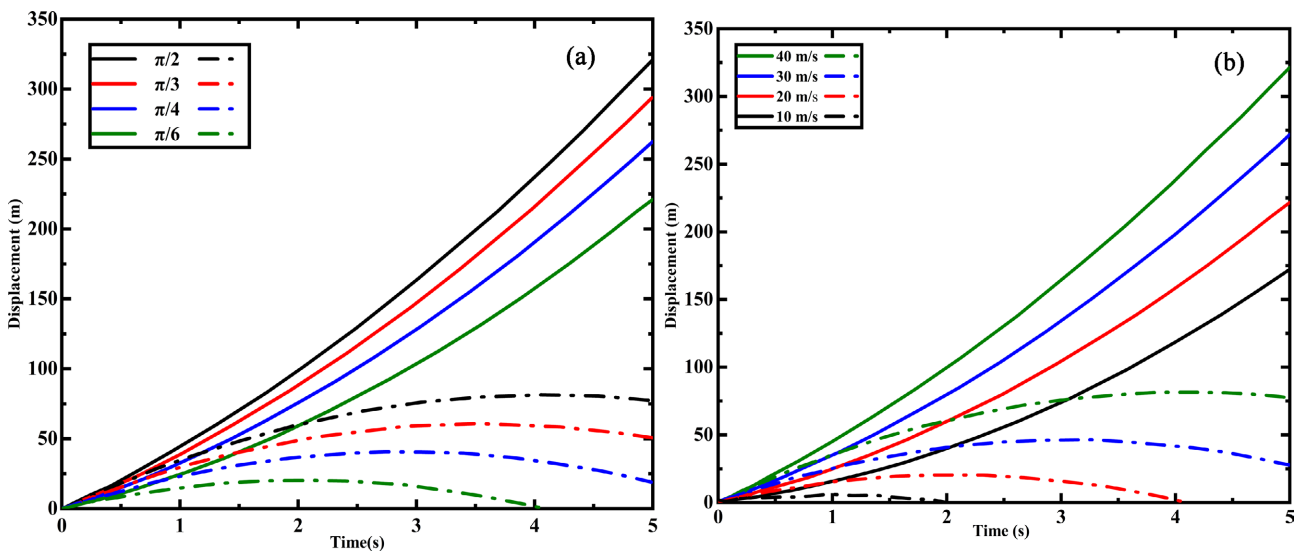


Figure 6. Comparison of vertical displacement between drag force (solid lines) and without drag force (dash-dot lines) with (a) variation on theta (θ) at $v = 40$ m/s. (b) Variation of initial velocity (v) at theta (θ) = $\pi/2$.

higher than that of (a) due to the increase of initial velocity.

3.3. Trajectory

The availability of exact analytical expressions of horizontal and vertical displacement as in Equations (11) and (18) respectively, allows plenty of features of the projectile motion in a linear air resistance to be confirmed. It also allows quantities and characteristics for the model of the trajectory of the projectile to be obtained in a trivial-like manner, sees [20]. As explained by Stewart [59] that, with the increase in projection angle (θ) and launched initial velocity (v_0), the trajectories of the projectile motions will be propagated more forwarded depending on those two factors (see Figure 7). The computation results of Equation (20) are presented in Figure 7. Our main goal in this section was to compare trajectories of projectile motion of varieties of inclined angle θ with different velocities.

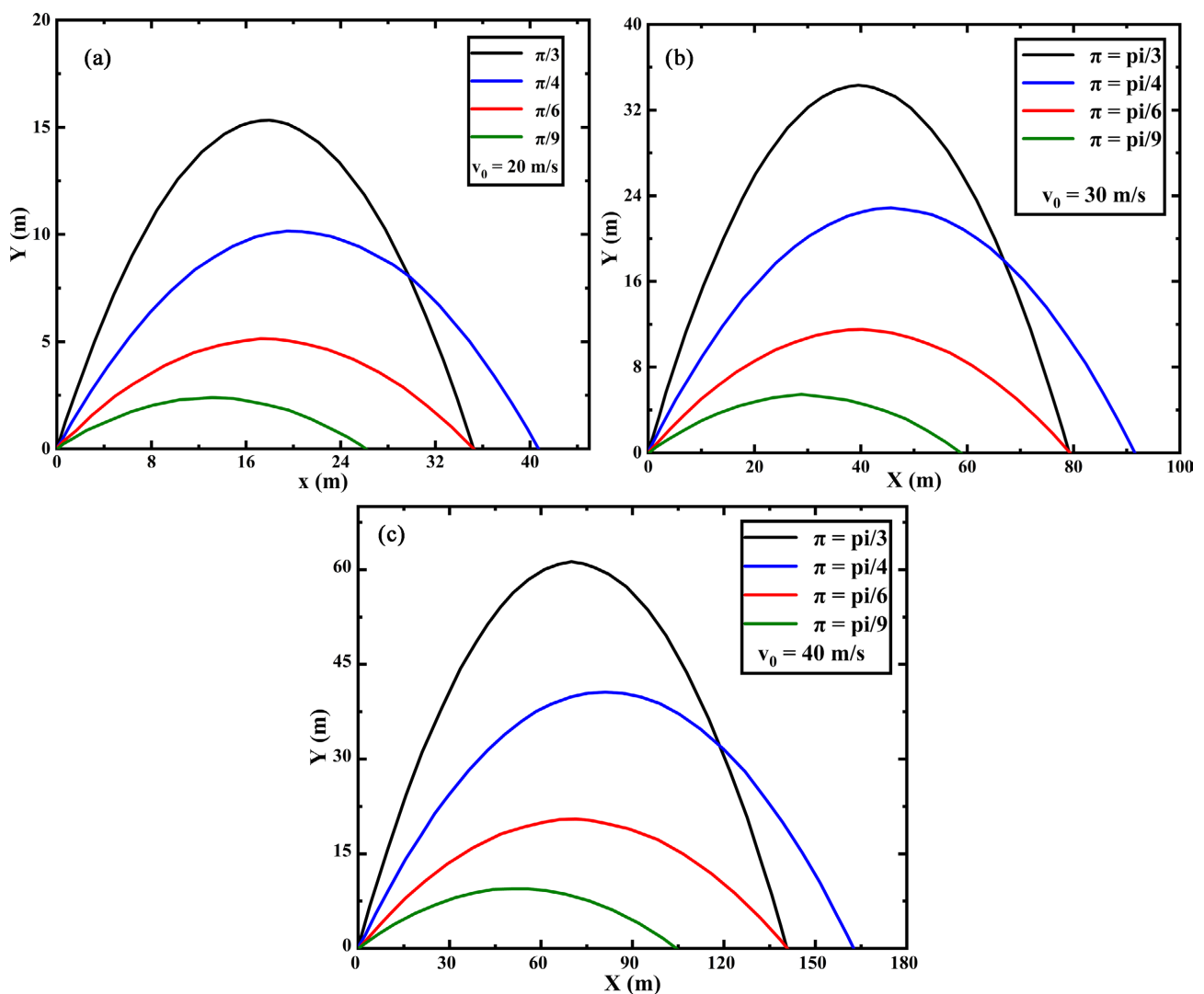


Figure 7. Trajectories of different launched theta (θ) with different initial velocities 20 m/s, 30 m/s, and 40 m/s as in (a), (b), and (c) respectively.

As illustrated in **Figure 7**, the maximum trajectory peak is attained by $\theta = \frac{\pi}{3}$ to all launched initial velocity (v_0) in (a), (b), and (c) respectively. This means that θ and v_0 are proportional to the trajectory (y (m)). It seems that, no matter what initial velocity (v_0) and theta (θ) induced in Equation (20), the results show that the best theta (θ) for the maximum range is always $\frac{\pi}{4}$. Our results give proof that the outlined trajectory by the projectile for the tossed angle theta (θ) is a segment of the parabola which is the same as it was described in [60]. The results also show that, for angle $\frac{\pi}{6}$ and $\frac{\pi}{3}$ with any sufficient initial velocity (v_0), there will be any point of intersection along $(x,0)$ while at $\frac{\pi}{3}$ and $\frac{\pi}{4}$ there will be an intersection point along (x,y) along the plane. Since in a vacuum, the projectile is launched with an initial velocity (v_0) at projection angle (θ) from the horizontal plane, then its trajectory can be found from its horizontal position as;

$$y(x) = x \tan \theta - \frac{1}{2} g \left(\frac{x^2}{v_0^2 \cos^2 \theta} \right) \quad (32)$$

Here, we compared the results from Equations (20) and (32) above by varying initial velocities 20 m/s, 30 m/s, 40 m/s, and 50 m/s with projection angle ($\theta = \frac{\pi}{6}$, $\frac{\pi}{4}$ and $\frac{\pi}{3}$ respectively. The results were traced using FreeMat and presented in **Figures 8-11** respectively. The red color shows the trajectories with air resistance (drag force) and the black color shows the trajectories without air resistance (vacuum). In each plot, the results show that the trajectories in a vacuum are higher than those with air resistance due to opposing force caused by drag force.

3.4. Range

The distance between horizontal displacement (x) when vertical displacement (y) is equal to zero refers to the range. Thus, the projectile travel in two distinct points along the horizontal direction, *i.e.*, it's the distance between the launched point and landing point of the projectile as in most of the basic physics books [61] [62].

The results from Equation (30) are presented in **Figure 12**. The results show that the range increase with the increase of velocity while the maximum range is attained when the projection angle (θ) is $\frac{\pi}{4}$. Theoretically, the range in a vacuum is greater than in the medium with air resistance due to the drag force acting upon the projectile as an opposing force.

4. Conclusion and Summary

The computational solution to the problem of projectile motion under significant

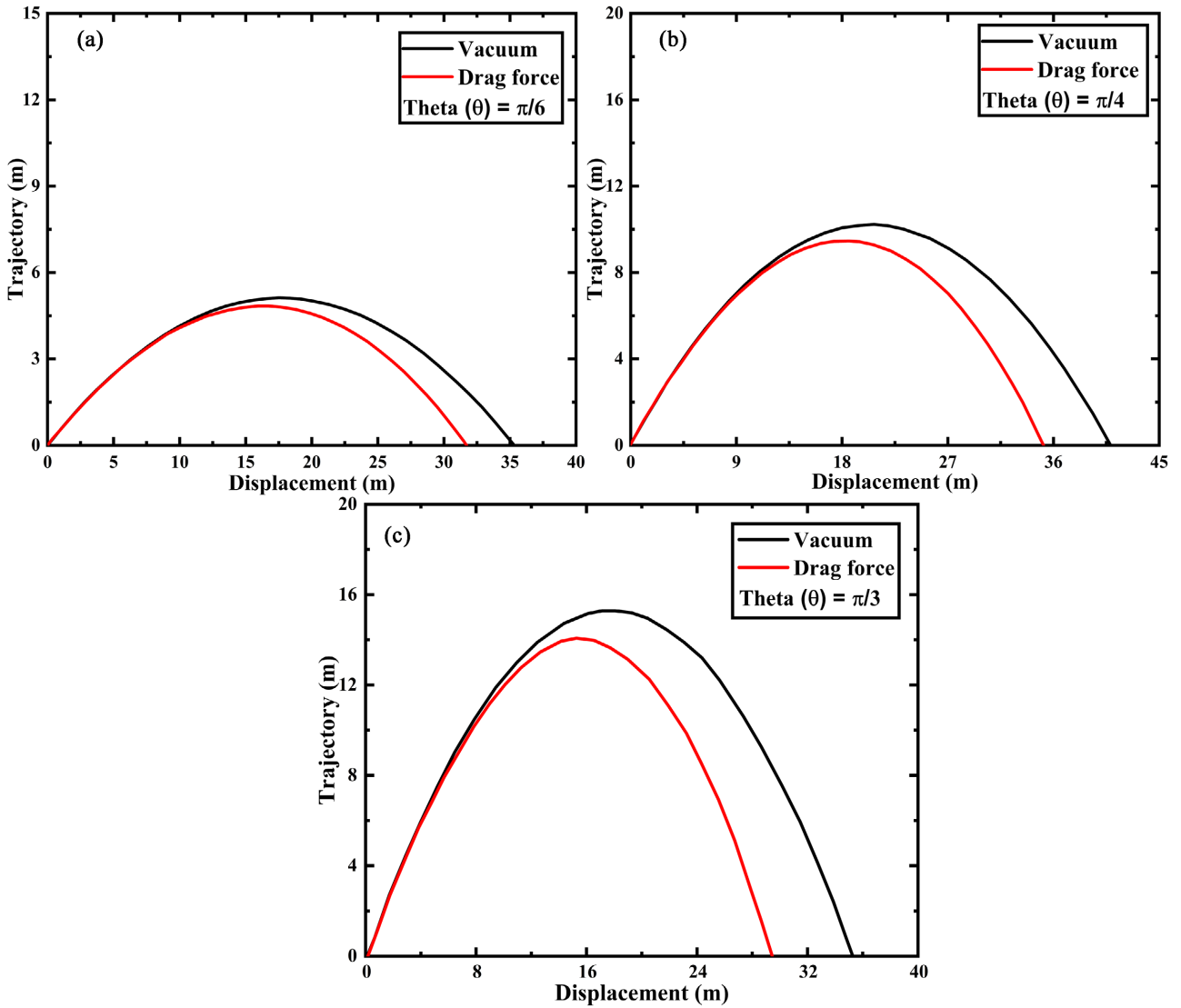
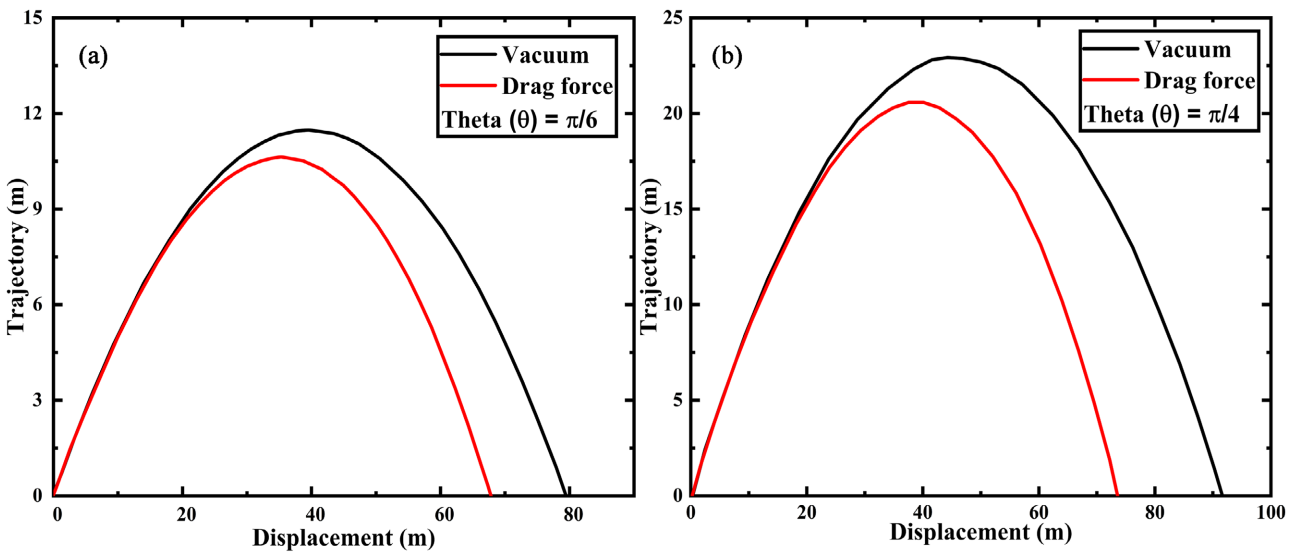


Figure 8. Trajectory with launched velocity 20 m/s.



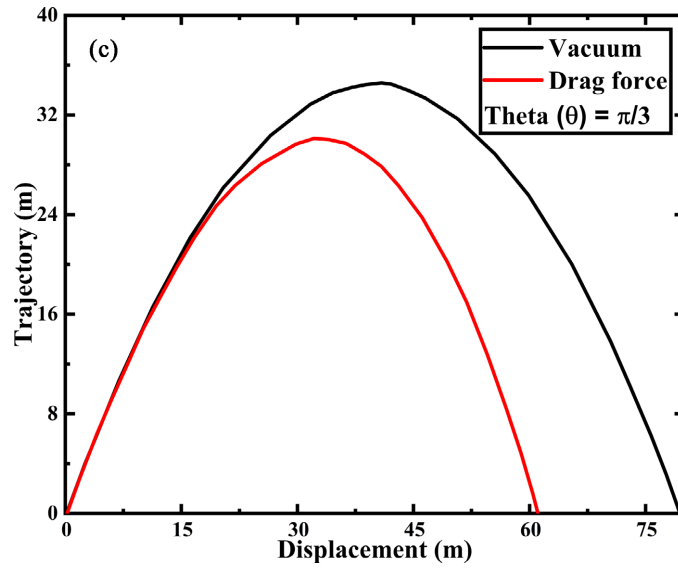


Figure 9. Trajectory with launched velocity 30 m/s.

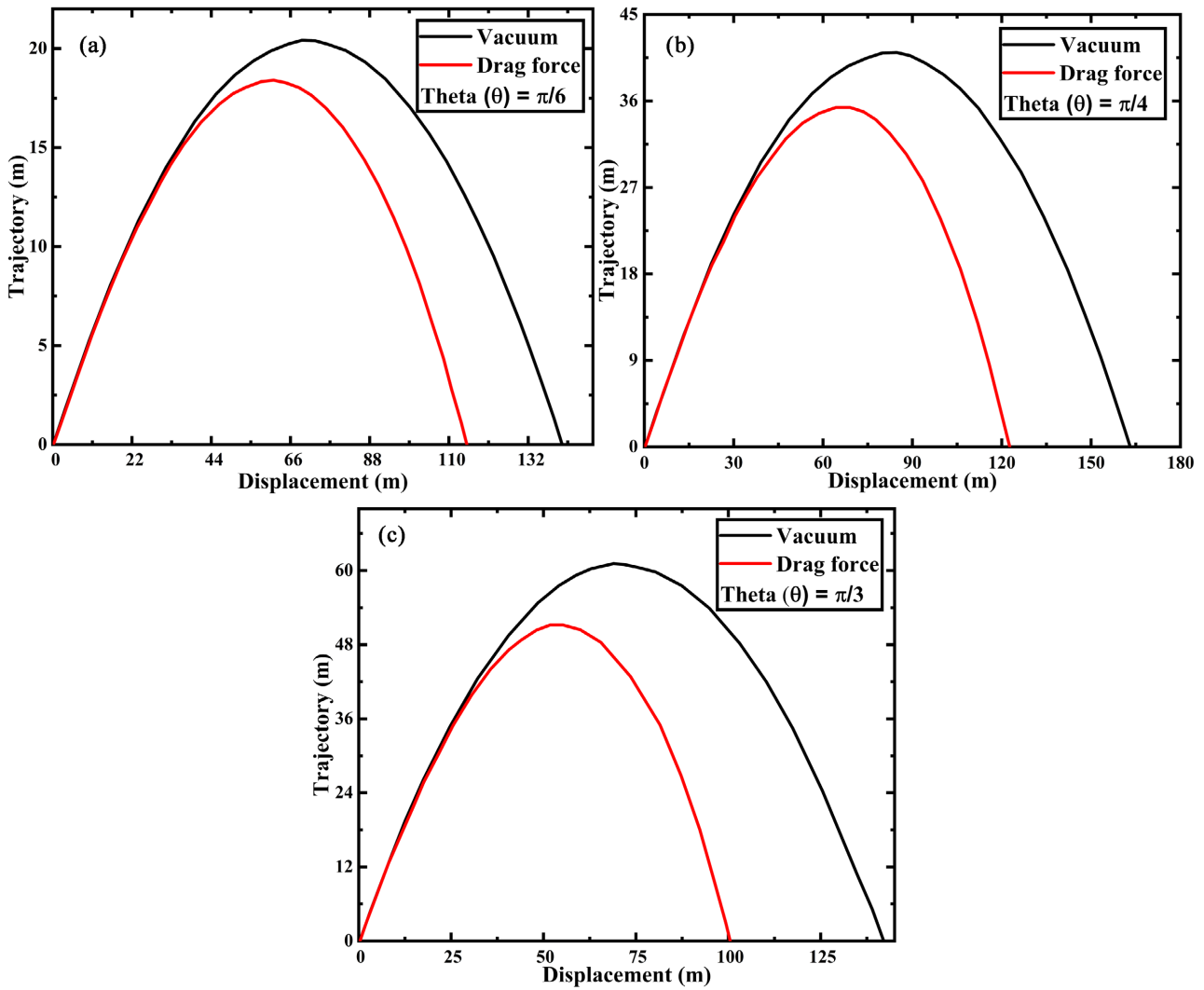


Figure 10. Trajectory with launched velocity 40 m/s.

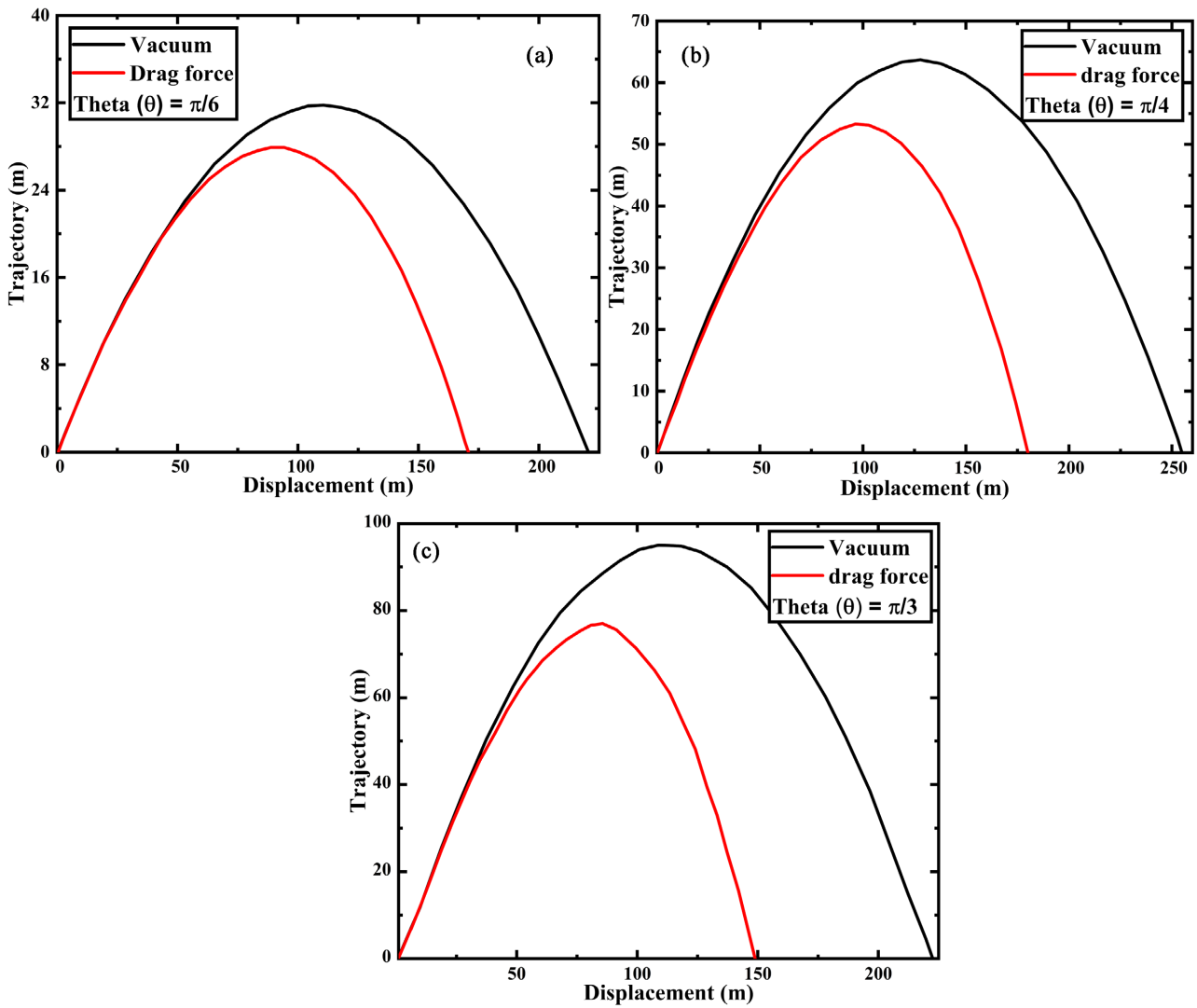


Figure 11. Trajectory with launched velocity 50 m/s.

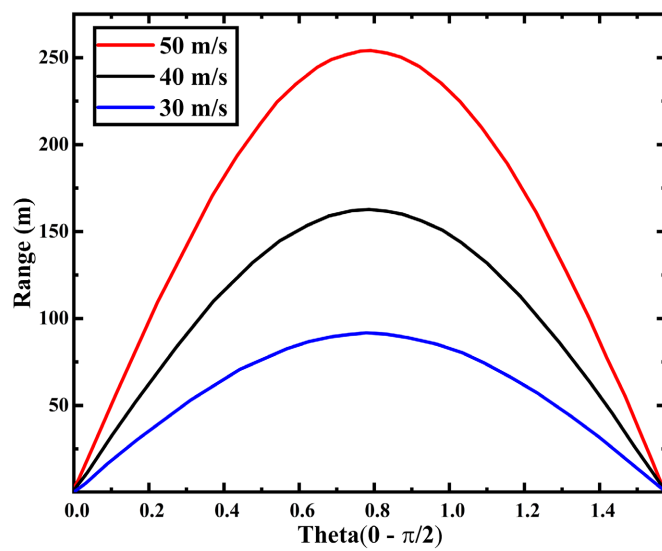


Figure 12. Range of projectile motion.

linear drag effect is critical to be known and evaluated. Therefore, based on this study, the following conclusion can be drawn;

1) The equations of motion under the effect of drag force (air resistance) were obtained by employing Newton's 2nd law of motion subjected to cartesian coordinates and employed to yield the horizontal and vertical component functions of projectile motion.

2) The algorithms for each function based on the STP conditions were generated and presented in detail. However, the study observed that the trajectory path of the projectile motion with linear drag force was found to be in a parabolic shape, **Figures 8-11**. This is due to the effect of gravity acting upon the projectile during the motion.

3) Similarly, the results showed that the effect of drag force causes the range of the projectile motion to be less compared to that in a vacuum.

4) Furthermore, the intensity of the drag force applied to the projectile motion under linear air resistance affects the results in both horizontal and vertical components of the motion compared to vacuum *i.e.*, the more the drag force the more the effect it causes to the projectile motion.

5) Finally, the simplicity and overall effectiveness of this model and functions derived in this work can serve an educational purpose and the scheme of this work will deal with the application for future study, especially to solutions of quadratic air resistance.

Acknowledgments

The authors acknowledge the support from the China University of Geosciences, Wuhan, China.

Data Availability Statement

All data can be obtained from the corresponding author upon request.

Conflicts of Interest

The authors declare no conflicts of interest regarding the publication of this paper.

References

- [1] Naylor, R.H. (1980) Galileo's Theory of Projectile Motion. *Isis*, **71**, 550-570. <https://doi.org/10.1086/352592>
- [2] Franco, A.B. (2003) Avempace, Projectile Motion and Impetus Theory. *Journal of the History of Ideas*, **64**, 521-546. <https://doi.org/10.1353/jhi.2004.0004>
- [3] Palmerino, C.R. (2004) Galileo's Theories of Free Fall and Projectile Motion as Interpreted by Pierre Gassendi. In: Palmerino, C.R. and Thijssen, J.M.M.H., Eds., *The Reception of the Galilean Science of Motion in Seventeenth-Century Europe, Boston Studies in the Philosophy of Science*, Vol. 239, Springer, Dordrecht, 137-164. https://doi.org/10.1007/978-1-4020-2455-9_8
- [4] Abattouy, M. (1996) Galileo's Manuscript 72: Genesis of the New Science of Motion

- (Padua, ca. 1600-1609). Ph.D. Thesis, Mohammed V University, Rabat.
- [5] Hooper, W. (1992) Galileo and the Problems of Motion. Ph.D. Thesis, Indiana University, Bloomington.
 - [6] Ebaid, A. (2011) Analysis of Projectile Motion in View of Fractional Calculus. *Applied Mathematical Modelling*, **35**, 1231-1239. <https://doi.org/10.1016/j.apm.2010.08.010>
 - [7] Charles Kittel, W.D.K. and Malvin, A. (1973) Ruderman, Mechanics. Second Edition, Vol. 1, McGraw-Hill, New York, 426.
 - [8] Ray, S. and Fröhlich, J. (2015) An Analytic Solution to the Equations of the Motion of a Point Mass with Quadratic Resistance and Generalizations. *Archive of Applied Mechanics*, **85**, 395-414. <https://doi.org/10.1007/s00419-014-0919-x>
 - [9] Parker, G. (1977) Projectile Motion with Air Resistance Quadratic in the Speed. *American Journal of Physics*, **45**, 606-610. <https://doi.org/10.1119/1.10812>
 - [10] Warburton, R. and Wang, J. (2010) Analytic Approximations of Projectile Motion with Quadratic Air Resistance. *Journal of Service Science and Management*, **3**, 98-105. <https://doi.org/10.1119/1.10812>
 - [11] Chudinov, P. (2001) The Motion of a Point Mass in a Medium with a Square Law of Drag. *Journal of Applied Mathematics and Mechanics*, **65**, 421-426. [https://doi.org/10.1016/S0021-8928\(01\)00047-8](https://doi.org/10.1016/S0021-8928(01)00047-8)
 - [12] Chudinov, P.S. (2003) Analytical Investigation of Point Mass Motion in Midair. *European Journal of Physics*, **25**, 73-79. <https://doi.org/10.1088/0143-0807/25/1/010>
 - [13] Turkyilmazoglu, M. (2016) Highly Accurate Analytic Formulae for Projectile Motion Subjected to Quadratic Drag. *European Journal of Physics*, **37**, Article ID: 035001. <https://doi.org/10.1088/0143-0807/37/3/035001>
 - [14] Cross, R. (2021) Vertical Bounce of a Spinning Ball. *Physics Education*, **56**, Article ID: 023002. <https://doi.org/10.1088/1361-6552/abd0d8>
 - [15] Nathan, A.M. (2008) The Effect of Spin on the Flight of a Baseball. *American Journal of Physics*, **76**, 119-124. <https://doi.org/10.1119/1.2805242>
 - [16] Robinson, G. and Robinson, I. (2013) The Motion of an Arbitrarily Rotating Spherical Projectile and Its Application to Ball Games. *Physica Scripta*, **88**, Article ID: 018101. <https://doi.org/10.1088/0031-8949/88/01/018101>
 - [17] Ilton, M., Bhamla, M.S., Ma, X., et al. (2018) The Principles of Cascading Power Limits in Small, Fast Biological and Engineered Systems. *Science*, **360**, eaao1082. <https://doi.org/10.1126/science.aao1082>
 - [18] Vogel, S. (2005) Living in a Physical World II. The Bio-Ballistics of Small Projectiles. *Journal of Biosciences*, **30**, 167-175. <https://doi.org/10.1007/BF02703696>
 - [19] Hu, H., Zhao, Y., Guo, Y.L. and Zheng, M.Y. (2012) Analysis of Linear Resisted Projectile Motion Using the Lambert W Function. *Acta Mechanica*, **223**, 441-447. <https://doi.org/10.1007/BF02703696>
 - [20] Stewart, S.M. (2006) An Analytic Approach to Projectile Motion in a Linear Resisting Medium. *International Journal of Mathematical Education in Science and Technology*, **37**, 411-431. <https://doi.org/10.1080/00207390600594911>
 - [21] Benacka, J. (2009) Simulating Projectile Motion in the Air with Spreadsheets. *Spreadsheets in Education (eJSiE)*, **3**, Article 3.
 - [22] Grigore, I., Miron, C. and Barna, E. (2017) Exploring Excel Spreadsheets to Simulate the Projectile Motion in the Gravitational Field. *Romanian Reports in Physics*, **69**, Article No. 901.

- [23] Cohen, C., Darbois-Textier, B., Dupeux, G., et al. (2014) The Aerodynamic Wall. *Proceedings of the Royal Society A: Mathematical, Physical and Engineering Sciences*, **470**, Article ID: 20130497. <https://doi.org/10.1098/rspa.2013.0497>
- [24] Hackborn, W.W. (2008) Projectile Motion: Resistance Is Fertile. *The American Mathematical Monthly*, **115**, 813-819. <https://doi.org/10.1080/00029890.2008.11920595>
- [25] Hackborn, W.W. (2016) On Motion in a Resisting Medium: A Historical Perspective. *American Journal of Physics*, **84**, 127-134. <https://doi.org/10.1119/1.4935896>
- [26] Watts, R.G. and Ferrer, R. (1987) The Lateral Force on a Spinning Sphere: Aerodynamics of a Curveball. *American Journal of Physics*, **55**, 40-44. <https://doi.org/10.1119/1.14969>
- [27] Allen, E. (2018) Approximate Ballistics Formulas for Spherical Pellets in Free Flight. *Defence Technology*, **14**, 1-11. <https://doi.org/10.1016/j.dt.2017.11.004>
- [28] Smith, L. and Sciacchitano, A. (2022) Baseball Drag Measurements in Free Flight. *Applied Sciences*, **12**, Article 1416. <https://doi.org/10.3390/app12031416>
- [29] Taylor, J. (2005) *Classical Mechanics*. University Science Books, Sausalito.
- [30] Fowles, G. and Cassiday, G. (2005) *Analytical Mechanics*. 7th Edition, Thomson Brooks/Cole, Belmont.
- [31] Lubarda, M.V. and Lubarda, V.A. (2022) Inelastic Bouncing of a Spherical Ball in the Presence of Quadratic Drag with Application to Sports Balls. *Proceedings of the Institution of Mechanical Engineers, Part P: Journal of Sports Engineering and Technology*. <https://doi.org/10.1177/17543371221086190>
- [32] Thornton, S.T. and Marion, J.B. (2021) *Classical Dynamics of Particles and Systems*. Cengage Learning, Boston.
- [33] Lubarda, M.V. and Lubarda, V.A. (2021) An Analysis of Pendulum Motion in the Presence of Quadratic and Linear Drag. *European Journal of Physics*, **42**, Article ID: 055014. <https://doi.org/10.1088/1361-6404/ac1446>
- [34] Hayen, J.C. (2003) Projectile Motion in a Resistant Medium: Part I: Exact Solution and Properties. *International Journal of Non-Linear Mechanics*, **38**, 357-369. [https://doi.org/10.1016/S0020-7462\(01\)00067-1](https://doi.org/10.1016/S0020-7462(01)00067-1)
- [35] Goff, J.E. (2013) A Review of Recent Research into Aerodynamics of Sport Projectiles. *Sports Engineering*, **16**, 137-154. <https://doi.org/10.1007/s12283-013-0117-z>
- [36] Jia, Q., Li, X., Song, J., et al. (2014) Projectile Motion Aerodynamic Parameter Identification and Simulation. *Proceedings of 2014 9th IEEE Conference on Industrial Electronics and Applications*, Hangzhou, 9-11 June 2014, 1872-1876. <https://doi.org/10.1109/ICIEA.2014.6931473>
- [37] Siegel, P. (2017) Using Statcast to Lift the Discussion of Projectile Motion. *American Journal of Physics*, **85**, 313-314. <https://doi.org/10.1119/1.4975302>
- [38] White, C. (2010) *Projectile Dynamics in Sport: Principles and Applications*. Routledge, London. <https://doi.org/10.4324/9780203885574>
- [39] Lubarda, M.V. and Lubarda, V.A. (2022) A Review of the Analysis of Wind-Influenced Projectile Motion in the Presence of Linear and Nonlinear Drag Force. *Archive of Applied Mechanics*, **92**, 1997-2017. <https://doi.org/10.1007/s00419-022-02173-7>
- [40] Milton, G.W. and Willis, J.R. (2007) On Modifications of Newton's Second Law and Linear Continuum Elastodynamics. *Proceedings of the Royal Society A: Mathematical, Physical and Engineering Sciences*, **463**, 855-880. <https://doi.org/10.1098/rspa.2006.1795>

- [41] Ivchenko, V. (2018) On Projectile Motion with Quadratic Drag Force. *European Journal of Physics*, **39**, Article ID: 045004. <https://doi.org/10.1088/1361-6404/aab343>
- [42] Yáñez-Valdez, R., Valdez, P. and Rivero, F. (2020) Horizontal Projectile Motion: Comparing Free Fall and Drag Resistance. *Revista Mexicana de Física E*, **17**, 156-164. <https://doi.org/10.31349/RevMexFisE.17.156>
- [43] Adair, R.K. (2001) Comment on “The Sweet Spot of a Baseball Bat,” by Rod Cross [Am. J. Phys. 66 (9), 772-779 (1998)]. *American Journal of Physics*, **69**, 229-230. <https://doi.org/10.1119/1.1286856>
- [44] Basu, S. (2011) FreeMat v4.1 Documentation. <https://sourceforge.net/projects/freemat/files/FreeMat4>
- [45] Coman, E., Brewster, M.W., Popuri, S.K., et al. (2012) A Comparative Evaluation of Matlab, Octave, FreeMat, Scilab, R and IDL on Tara. UMBC Faculty Collection.
- [46] Glavelis, T., Ploskas, N. and Samaras, N. (2010) A Computational Evaluation of Some Free Mathematical Software for Scientific Computing. *Journal of Computational Science*, **1**, 150-158. <https://doi.org/10.1016/j.jocs.2010.06.002>
- [47] Sharma, N. and Gobbert, M.K. (2010) A Comparative Evaluation of Matlab, Octave, FreeMat and Scilab for Research and Teaching. UMBC Faculty Collection.
- [48] Dhanemozhi, A.C. (2015) Projectile Motion Using Matlab. *International Journal of Science, Technology & Management*, **4**, 1103-1107.
- [49] Miranda, E., Nikolskaya, S. and Riba, R. (2012) Minimum and Terminal Velocities in Projectile Motion. *Revista Brasileira de Ensino de Física*, **26**, 125-127. <https://doi.org/10.1590/S1806-11172004000200007>
- [50] (2007) Taylor Series Expansions. In: Heidergott, B., Ed., *Max-Plus Linear Stochastic Systems and Perturbation Analysis, The International Series on Discrete Event Dynamic Systems*, Vol. 15, Springer, Boston, 179-263.
- [51] Demir, A., Erman, S., Özgür, B., et al. (2013) Analysis of Fractional Partial Differential Equations by Taylor Series Expansion. *Boundary Value Problems*, **2013**, Article No. 68. <https://doi.org/10.1186/1687-2770-2013-68>
- [52] Masjed-Jamei, M., Moalemi, Z., Area, I., et al. (2018) A New Type of Taylor Series Expansion. *Journal of Inequalities and Applications*, **2018**, Article No. 116. <https://doi.org/10.1186/s13660-018-1709-8>
- [53] Wu, Y. and Litmanovich, Y.A. (2020) Strapdown Attitude Computation: Functional Iterative Integration versus Taylor Series Expansion. *Gyroscopy and Navigation*, **11**, 263-276. <https://doi.org/10.1134/S2075108720040124>
- [54] Groetsch, C.W. and Cipra, B. (1997) Halley’s Comment—Projectiles with Linear Resistance. *Mathematics Magazine*, **70**, 273-280. <https://doi.org/10.1080/0025570X.1997.11996553>
- [55] Hecht, H. and Bertamini, M. (2000) Understanding Projectile Acceleration. *Journal of Experimental Psychology: Human Perception and Performance*, **26**, 730-746. <https://doi.org/10.1037/0096-1523.26.2.730>
- [56] Runeson, S. (1974) Constant Velocity—Not Perceived as such. *Psychological Research*, **37**, 3-23. <https://doi.org/10.1007/BF00309076>
- [57] Buček, S. (2016) Falling Objects and Projectile Motion with Regard the Air Resistance. *Proceedings of 8th International Conference on Education and New Learning Technologies*, Barcelona, 4-6 July 2016, 8243-8249. <https://doi.org/10.21125/edulearn.2016.0800>
- [58] Moon, G.-H., Tahk, M.-J., Han, D.H. and Son, J.Y. (2021) Generalized Polynomial

Guidance for Terminal Velocity Control of Tactical Ballistic Missiles. *International Journal of Aeronautical and Space Sciences*, **22**, 163-175.

<https://doi.org/10.1007/s42405-020-00291-6>

- [59] Stewart, S. (2006) Characteristics of the Trajectory of a Projectile in a Linear Resisting Medium and the Lambert W Function. *Proceedings of Australian Institute of Physics 17th National Congress*, Brisbane, 3-8 December 2006, 1-4.
- [60] Kantrowitz, R. and Neumann, M.M. (2014) Some Real Analysis behind Optimization of Projectile Motion. *Mediterranean Journal of Mathematics*, **11**, 1081-1097.
<https://doi.org/10.1007/s00009-013-0379-5>
- [61] Riley, K.F., Hobson, M.P. and Bence, S.J. (1999) Mathematical Methods for Physics and Engineering. *American Journal of Physics*, **67**, 165-169.
<https://doi.org/10.1119/1.19216>
- [62] Verma, H.C. (1993) Concepts of Physics. Bharati Bhawan.